Aerosol and Air Quality Research, 16: 2692–2705, 2016

ISSN: 1680-8584 print / 2071-1409 online
doi: 10.4209/aaqr.2015.07.0455

Correlation Analysis, Transportation Mode of Atmospheric Mercury and Criteria Air Pollutants, with Meteorological Parameters at Two Remote Sites of Mountain and Offshore Island in Asia

Wang-Kun Chen[1], Tsung-Chang Li[2], Guey-Rong Sheu[3], Neng-Huei Lin[3], Liang-Yu Chen[4*], Chung-Shin Yuan[2*]

[1] *Department of Environment and Property Management, Jinwen University of Science and Technology, New Taipei 23154, Taiwan*
[2] *Institute of Environmental Engineering, National Sun-Yat Sen University, Kaohsiung 80424, Taiwan*
[3] *Department of Atmospheric Sciences, National Central University, Chung-Li 32001, Taiwan*
[4] *Department of Biotechnology, Ming-Chuan University, Taoyuan 33343, Taiwan*

ABSTRACT

This study presents a comparison of trace (Hg) and criteria (CO, SO_2, NO_x, O_3 and PM_{10}) air pollutants monitored at two remote sites with the same latitude but different altitude: Mt. Lulin and the Penghu Islands, in Taiwan from 2011 to 2012. A filtering technique was comprehensively applied to distinguish the climatic characteristics of the two remote sites, as well as to determine their discriminant factor. The concentrations of air pollutants monitored at Mt. Lulin were generally lower than those at the Penghu Islands, with the exception of O_3 concentration. PM_{10} and NO_x were the important factors that can distinguish two clusters of measurement data at the two remote sites, and a criteria discriminant factor of atmospheric parameters derived from these two air pollutants. For both high- and low-frequency patterns, the concentrations of NO_x and PM_{10} exhibit significant differences between the two remote sites. However, O_3 concentrations showed almost no differences between these two remote sites, implying that the pattern for the formation and transportation of O_3 at these two sites resulted from similar mechanisms. Moreover, atmospheric mercury (TGM) had a very good linear correlation with CO. The diurnal variation of Hg concentration was dramatic at the Penghu Islands, while it appeared as low as the North Hemisphere background mercury concentration at Mt. Lulin, indicating that they were not formed via the mechanism modes. This study thus proposed "scenario mercury" and "background mercury" for interpreting this interesting phenomenon.

Keywords: Remote sites; Atmospheric mercury; Criteria air pollutants; Meteorological parameters; Correlation and transportation.

INTRODUCTION

Global monitoring of trace and criteria air pollutants at remote sites has been widely undertaken over the past decades (Fu *et al.*, 2008, 2009; Sheu *et al.*, 2010; Nguyen *et al.*, 2010; Ci *et al.*, 2011; Pfaffhuber *et al.*, 2012; Cole *et al.*, 2013; Sheu *et al.*, 2013; Kumari *et al.*, 2015). The remote sites were set up to cover the in-land continents and offshore islands worldwide (Fu *et al.*, 2012; Sheu *et al.*, 2013; Jen *et al.*, 2014). These remote air quality monitoring sites were established mostly to collect long-term background levels of air pollutants that are transported globally, including continent-continent and ocean-continent cross-boundary transports (Lin and Pehkonen, 1999; Cheng and Hu, 2010; Durnford *et al.*, 2010). Compared to the local sources, the remote background sites have the advantages of less influences of anthropogenic air pollution and high representative of upwind background air quality.

Background trace and criteria air pollutants are monitored long-term at these remote sampling sites. Except for a few sites used as local sampling stations, most of them are treated as long-range transportation and/or background air quality monitoring sites (Ci *et al.*, 2011; Fu *et al.*, 2012; Sheu *et al.*, 2013; Jen *et al.*, 2014). In addition to the criteria air pollutants, including CO, SO_2, NO_x, O_3, $PM_{2.5}$ and PM_{10}, the trace air pollutants mainly cover suspended particles, heavy metals, polycyclic aromatic hydrocarbons (PAHs), dioxins, etc. (Schroeder and Munthe, 1998; Pal and Ariya, 2004a; Leonardo *et al.*, 2007; Fu *et al.*, 2010; Sommar *et al.*, 2010).

* Corresponding author.
Tel.: 886-7-5252000 ext. 4409; Fax: 886-7-5254449
E-mail address: ycsngi@mail.nsysu.edu.tw

Among the heavy metals, mercury is a unique metal of liquid phase; it has attracted great interest owing to its toxicity and long lifespan in the atmosphere (Schroeder and Munthe, 1998). Moreover, atmospheric mercury pollution has been deemed as the second important global environmental issue following the greenhouse effects (UNEP, 2008). Atmospheric mercury comprises gaseous elemental mercury (GEM), gaseous oxidized mercury (GOM) and particulate mercury (PHg); they are mostly present as gaseous elemental mercury in the atmosphere (Lin and Pehkonen, 1999). The main sources of mercury emitted into the atmospheric environment include fuel and waste combustion, mining and smelting operations, biomass burning and industrial processes (Pacyna *et al.*, 2006; Wu *et al.*, 2012; Jen *et al.*, 2013).

Due to the long lifetime (0.5–2 years) of GEM in the atmosphere, it has become more interesting for scientists and government agencies; hence, it is vital to understand its transportation phenomena (Slemer and Langer, 1992; Schroeder, W. H. and J. Munthe, 1998). Its influences are not restricted to the areas of mercury emission sources, as it could also be transported long distance to a downwind region (Bash *et al.*, 2007; Ci *et al.*, 2011). High mercury concentration has been observed in places far away from its anthropogenic sources (Fitzgerald *et al.*, 1998).

In recent years, there has been a tremendous focus on global environmental pollution problems caused by atmospheric mercury. Mercury mainly emerges from combustion processes; however, the atmospheric dispersion makes its transport a worldwide phenomenon due to its long lifetime in the atmosphere. In the past decade, a great deal of research has been devoted to investigating mercury transportation and its emission sources (Fang *et al.*, 2001; Wang *et al.*, 2006; Fu *et al.*, 2009; Kim *et al.*, 2012; Choi *et al.*, 2013; Liu *et al.*, 2014). Modeling the emission sources of mercury has been conducted in the UK, based on emission data from the 1990's. The results emphasized that around 40% of mercury monitored in the UK is emitted from local UK sources, 25% came from the global background, while the rest 33% were from other European countries (Lee *et al.*, 2001).

Previous studies focused on the mercury transportation between two sites but failed to elaborate on the physical properties of how mercury is transported in the atmosphere, especially in mountainous areas (Civerlo *et al.*, 2014); less work has been conducted in ascertaining the transport pattern of atmospheric mercury.

Therefore, this study aims to carry out correlation analysis and investigate the transportation modes of atmospheric mercury at two sites: a remote mountain and an off-shore island in seeking possible mechanisms for chemical conversions of air pollutants as well as meteorological parameters measured at the two remote sites. The transportation phenomenon of mercury was also investigated in this study.

EXPERIMENTAL METHODS

Sampling Sites

The locations of two remote sites investigated in this study are shown in Fig. 1. Mt. Lulin Meteorological Station is located at the intersection of Nantou and Chiayi Counties

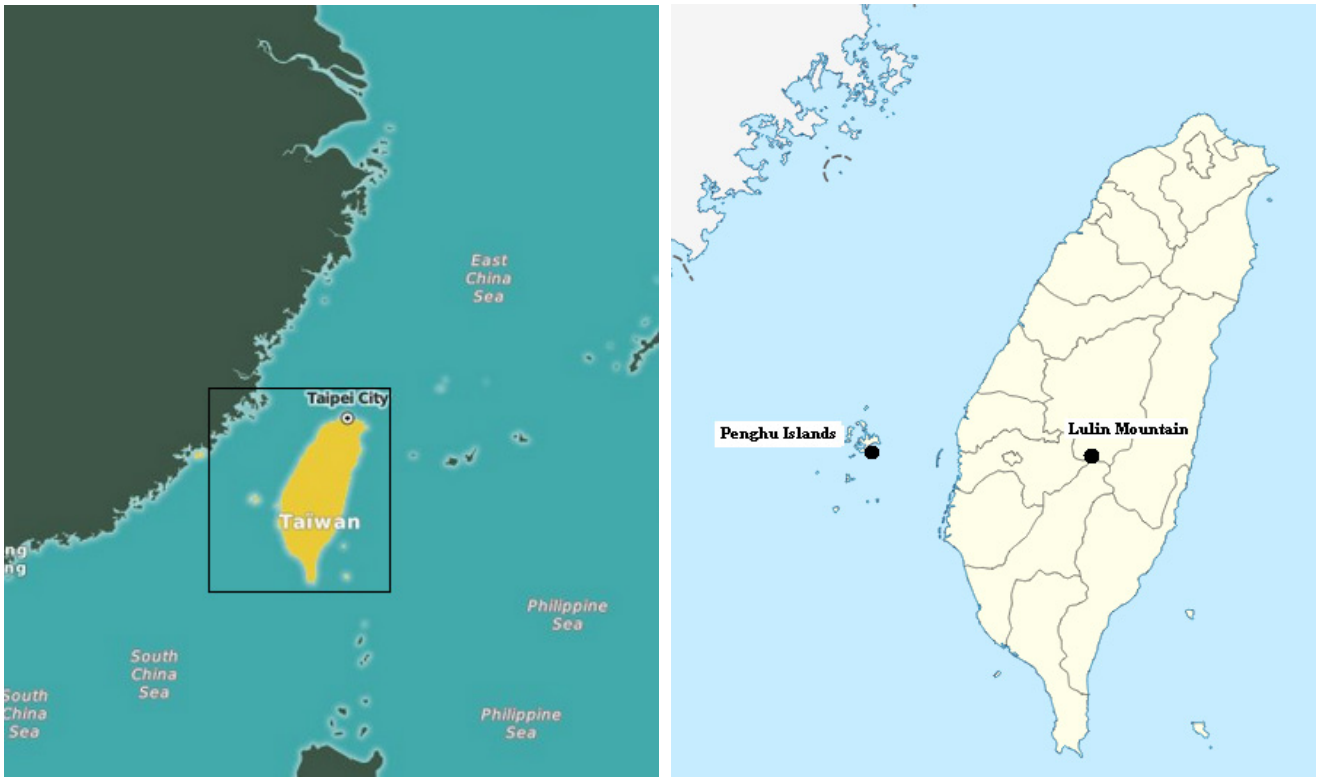

Fig. 1. Location of two subtropical remote sites in Taiwan.

in Central Taiwan with the longitude of 120°52'25"E and Latitude of 23°28'07"N, and altitude of 2,862 m. This station is considered as a global mountainous background site for atmospheric chemistry monitoring. The Penghu Air Quality Sampling Station is located on the Penghu Islands, situated in the middle of the Taiwan Strait (Jen *et al.*, 2014).

The two stations investigated in this study are on the same latitude but their elevation and geographical environments are totally different. As a background site, the Mt. Lulin Station is surrounded by high mountains with absolutely no anthropogenic sources. The Penghu Air Quality Sampling Station is located in suburban Makung City with a few anthropogenic sources, mainly automobiles and fishing boats. It is situated on the Penghu Islands right on the pathway of long-range transport between mainland China and Taiwan Island. The field monitoring of atmospheric mercury, criteria air pollutants and meteorological parameters during the four seasons was undertaken from March 2011 to February 2012. The data on ambient air quality and meteorological parameters monitored at the two remote sites were further applied to the correlation analysis, to investigate the transportation modes between these two remote sites. In this study, PM_{10} concentrations were routinely measured by automatic β-gauge monitors, which is in accordance with the US EPA-designated equivalent methods (No. EQPM-0391-081). The PM_{10} inlet is a cyclone operated at the sampling flow rate of 18.9 L min^{-1}. Gaseous air pollutants were monitored by the Taiwan Air Quality Monitoring Network (TAQMN). A monitoring protocol of ambient gaseous air pollutants including O_3, SO_2, CO and NO_x was conducted instrumentally at 3 m level above the ground.

Statistical Analysis of Monitoring Data

Visible analytical tools were used to determine the pattern in the monitored data set, and to find the correlation and mechanisms of transportation. Period filtering was further used in this study to resolve the characteristics of the natural environments and contamination properties with high and low frequencies. The main scope of pollutant transportation can be obtained with a statistical time series diagram. Several statistical tools were also applied to identify the characteristics of transportation patterns between the two remote sites. These include correlation analysis, frequency distribution and discriminant factor, which are described below.

Correlation Analysis

Correlation analysis provides information regarding independent variables of the distribution of two pollutants. The pollution concentration can be regarded as a random variable, and the correlation coefficient calculates the statistical relationship between these sets of data. However, it does not present the causal relationship of these pollutant concentrations. It only refers to the mathematical condition of probabilistic independence. The associated changes are illustrated in the time series diagram.

Time Series Analysis

Drawing the concentration changes of two separate monitoring stations via time series pattern can effectively exhibit the relative changes at each site. Causality between the two separate sites can be found by using the time series graphs. If the event of concentration changes appears at one site prior to the other site, then it can be interpreted that there is a considerable degree of causal relationship between each the sampling sites. Predicting pollutant concentration changes can thus be accomplished through the time series graphs.

The "low frequency" and "high frequency" are characterized by the time periods, which include daily, weekly, monthly, and seasonal variation patterns. The benefits for separately investigating the low- and high-frequency wave pattern of air pollutant concentrations were mainly applied to clarify the temporal variation patterns of air pollutants monitored at these two remote sites.

Frequency Distribution Analysis

Frequency distribution analysis presents a group of pollutant concentrations clustered into restricted groups, as well as the number of occurrences within the range. As the high- and low-frequency signals were mixed together in the monitoring results, this analytical scheme aided us in clarifying the contribution from these two frequency signals.

The most commonly used illustrated graphs are histograms, line charts, bar charts, pie charts, etc.; they are a convenient way to demonstrate the unorganized measured pollution concentration data. In this study, the frequency distribution was used for qualitative and quantitative data analysis. The indices related to frequency distribution include frequencies, relative frequency, cumulative frequency, etc., with different requirements for each distribution.

Climate Features

"Low frequency" and "high frequency" are characterized by the cycle time of the wave, which includes daily, weekly, monthly and seasonal variation patterns. The benefits of separately investigating the low- and high-frequency wave pattern of air pollutant concentrations were mainly applied to clarify the temporal variation patterns of air pollutants monitored at these two remote sites.

Changes in the low-frequency pattern of pollutant concentrations are mainly observed in the monthly or seasonal variation of pollutants. Low-frequency presents variations of contaminants as a result of climate factors which are mainly attributed from the influence of large-scale weather patterns. In addition, long-term climate change is also a concern in the low-frequency range. The natural environmental factors, such as ambient temperature, relative humidity, wind direction and wind speed must be intensively considered due to their high frequency influences, since they greatly impact on the concentration variation.

Weather Features

The high-frequency pattern refers to periods shorter than one day, which means that the periodic event is shorter. The variation of air pollutant concentration within a day or an hour is regarded as being within this category. Owing to the effects of heat radiation from sunlight and radiant cooling, the high-frequency changes become relatively important.

Due to the obvious diurnal variation in ambient temperature and the wide variations in the wind direction and wind speed, the transportation of air pollutants is greatly affected.

Discrimination Analysis

The index of discrimination is used to reflect the extent of differences between the behaviors of two pollutant concentrations. There are many ways to calculate the discrimination index, including the determination of the statistical significance of differences between two pollutant concentrations. The discrimination index can also be noted from the concentration profile of the pollutants; thus, the discrimination index of pollutant concentrations obtained from the two remote sites were further investigated in this study.

Pattern Recognition

Pattern recognition provides a good tool for understanding atmospheric transportation phenomena. There are many different methods of pattern recognition, and time series is one of the suitable tools. The time series technique with principle component analysis was used to determine the pattern of data measured at these two sites. The time variation and standard distribution of each pollutant was analyzed. We figured out the pattern of atmospheric transportation of mercury at these two remote sites by using the high- and low-frequency time series graphs, respectively. The information presented in the figures is sufficient to explain the characteristic of these two remote sites.

RESULTS AND DISCUSSION

Comparison of High-Frequency Features

The meteorological parameters monitored at the two remote sites were important factors affecting the transportation of various air pollutants. The comparison of hourly variation of ambient temperature, relative humidity, wind speed and suspended particles (PM_{10}) at the two remote sites are illustrated in Fig. 2. As a criteria air pollutant in the ambient air quality standard, PM_{10} is an important index to reveal the pollutant behavior during the transportation process. As PM_{10} may exist in the natural environment and/or emerge from anthropogenic sources, the measuring results of particulate matter were also included in Fig. 2(e).

The two-day short-term variations of air pollutants were also compared in Fig. 2. Hourly meteorological data are plotted for two specific dates in autumn. From the changes in the ambient temperature, it was observed that ambient temperatures at the Penghu Islands were higher and relatively more stable than those at Mt. Lulin (Fig. 2(a)). The maximum ambient temperature of the Penghu Islands occurred at noon, while the maximum ambient temperature at Mt. Lulin appeared between 9:00–10:00 in the morning; its temperature was much lower than that at the Penghu Island. Besides, fogs commonly occurred in the afternoon (2:00–4:00 pm) at Mt. Lulin, which blocked the irradiation of sunlight and reduced the ambient temperature. Thus, the ambient temperatures of the mountainous site generally increased in the morning and then decreased when fogs formed in the afternoon. The meteorological conditions (i.e., wind direction, wind speed and relative humidity) commonly varied drastically at Mt. Lulin, while they were relatively stable at the Penghu Islands (Figs. 2(b) –2(d)).

While the concentrations of PM_{10} appeared to be higher at the Penghu Islands, its value was much lower and variable at Mt. Lulin (Fig. 2(e)). A previous study used surface wind modeling to simulate the air masses transportation in the Penghu Islands domain. The results of the surface wind field showed that both prevailing winds and sea-land breezes highly influenced the surface wind fields at the Penghu Islands (Li *et al.*, 2015). Consequently, PM_{10} could be emitted from local sources and form by atmospheric chemical reactions (i.e., secondary aerosols), or may have resulted from long-range transportation during the prevailing wind periods. In comparing the concentrations of PM_{10} observed at the two remote sites, it was higher at the Penghu Islands, and included primary and secondary pollutants (Jeh *et al.*, 2014; Li *et al.*, 2015). At Mt. Lulin, it was more likely to be secondary pollutants derived mainly from atmospheric chemical reactions (Sheu *et al.*, 2010; Lee *et al.*, 2011; Chuang *et al.*, 2014).

Comparison of Low-Frequency Features

In addition to the daily variation of high-frequency, the seasonal low-frequency variation is depicted in Fig. 3. As shown in Fig. 3, low and stable ambient temperatures appeared at Mt. Lulin, while relatively high ambient temperatures were generally observed at the Penghu Islands. This is mainly attributed to the fact that the two remote sites are located at different altitutes above sea level. Ambient air temperatures have a tendency to decrease with height, following the lapse rate in the troposphere. The seasonal variation of ambient temperatures at these two remote sites showed a rather consistent pattern, higher in summer and lower in winter (Fig. 3(a)). This clearly demonstrated the similar climatic characteristics at the same latitude. In terms of the meteorological parameters, there was no significant difference in relative humidity between these two remote sites. Relative humidity was relatively stable at the Penghu Islands, showing the characteristics of island climate in the marine boundary layer, as shown in Fig. 3(b); however, a more dramatic change of relative humidity was observed at Mt. Lulin due to the typical subtropic mountain climate.

Comparing the wind speed monitored at these two remote sites, the Penghu Islands had higher wind speeds than those at Mt. Lulin and occasionally with stronger winds (Fig. 3(c)). The main impact of high wind speeds is its capability to transport air pollutants toward the downwind region. The sources of Hg do not appear near the two remote sites. Similar to other air pollutants, such as SO_2 and NO_x, mercury may also come from cross-boundary transport and local emission at the Penghu Islands (Jen *et al.*, 2014), while mostly arriving via cross-boundary transport from East Asia (Sheu *et al.*, 2013). CO comes mainly from traffic sources, and very few such sources exist near these two remote sites. For O_3, there is no primary source close to the monitoring stations, so it can be explained as secondary pollutant transported from other regions.

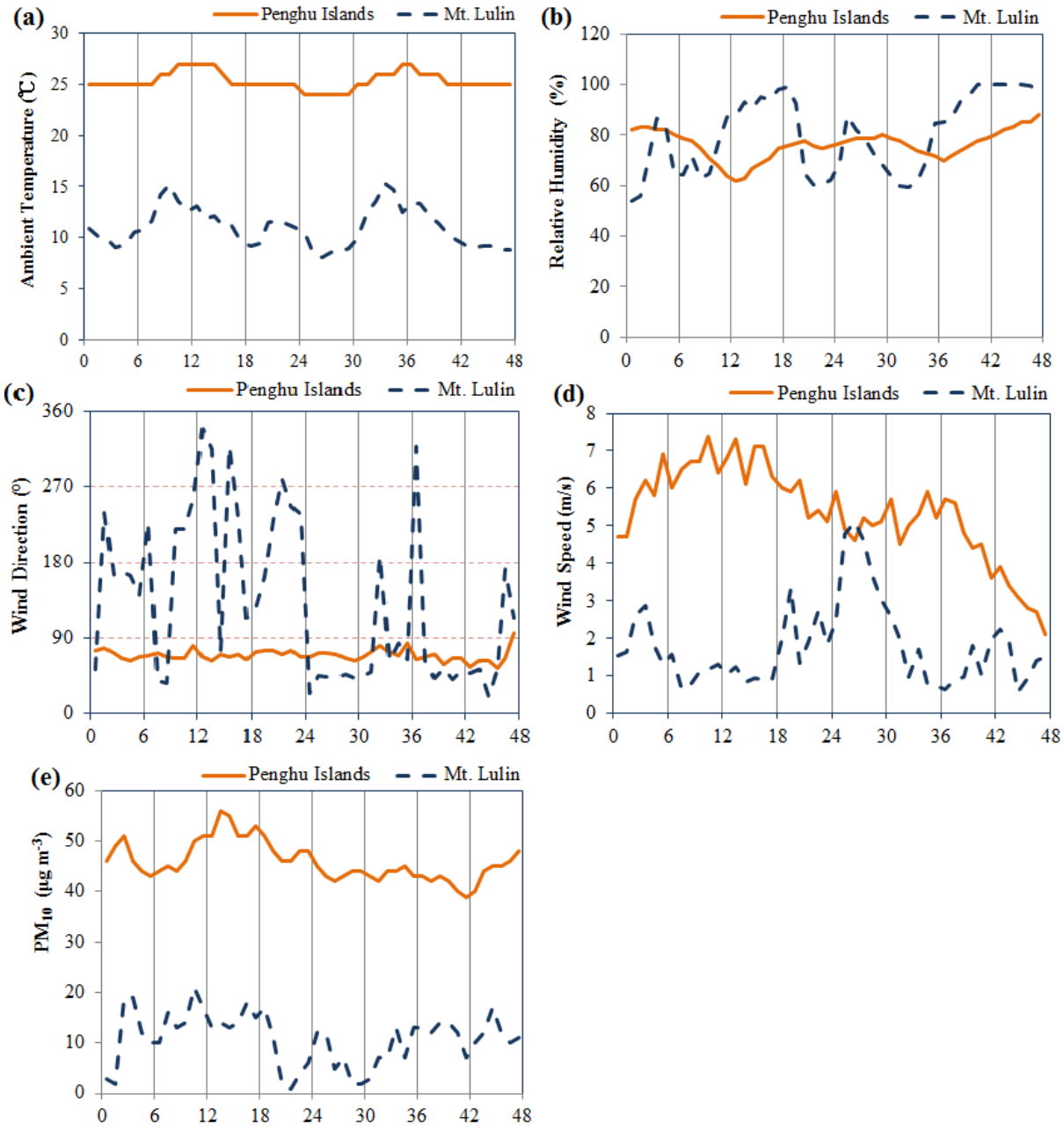

Fig. 2. Hourly variation of (a) ambient temperature, (b) relative humidity, (c) wind direction, (d) wind speed, (e) PM_{10}. The solid line (—) represents the Penghu Islands and the dash line (- - -) represents the Mt. Lulin.

The concentration levels of PM_{10} monitored at the Penghu Islands were generally higher and much more varied than those at Mt. Lulin, which was highly affected by the emissions of air pollutants from mobile sources (i.e., automobiles and fishing boats) at the Penghu Islands (Fig. 3(d)) (Yuan *et al.*, 2004a, b). Moreover, the topographies of these two remote stations differ greatly.

Air Pollutant Transportation Pattern

High Frequency Features of Air Pollutant Concentration

Hourly variation of air pollutants, including SO_2, NO_x, CO and O_3, in two consecutive days at the two remote sites are illustrated in Fig. 4. It shows that the trends of SO_2 levels observed at the two remote sites were quite similar, except that the levels of SO_2 at Mt. Lulin were lower than those at the Penghu Islands (Fig. 4(a)). The results support the point of view that the mechanism of SO_2 was mostly similar at the two remote sites. SO_2 is mainly formed and emitted from the combustion of sulfur-containing fuels. It could be transported downward in the atmosphere by dispersion and advection. Major combustion sources located in Taiwan and southeastern China could be the potential sources of SO_2 for these two remote sites.

The distribution trends of NO_x at the two remote sites also differed, with lower NO_x levels at Mt. Lulin (Fig. 4(b)). The emission of NO_x comes mainly from fuel combustion

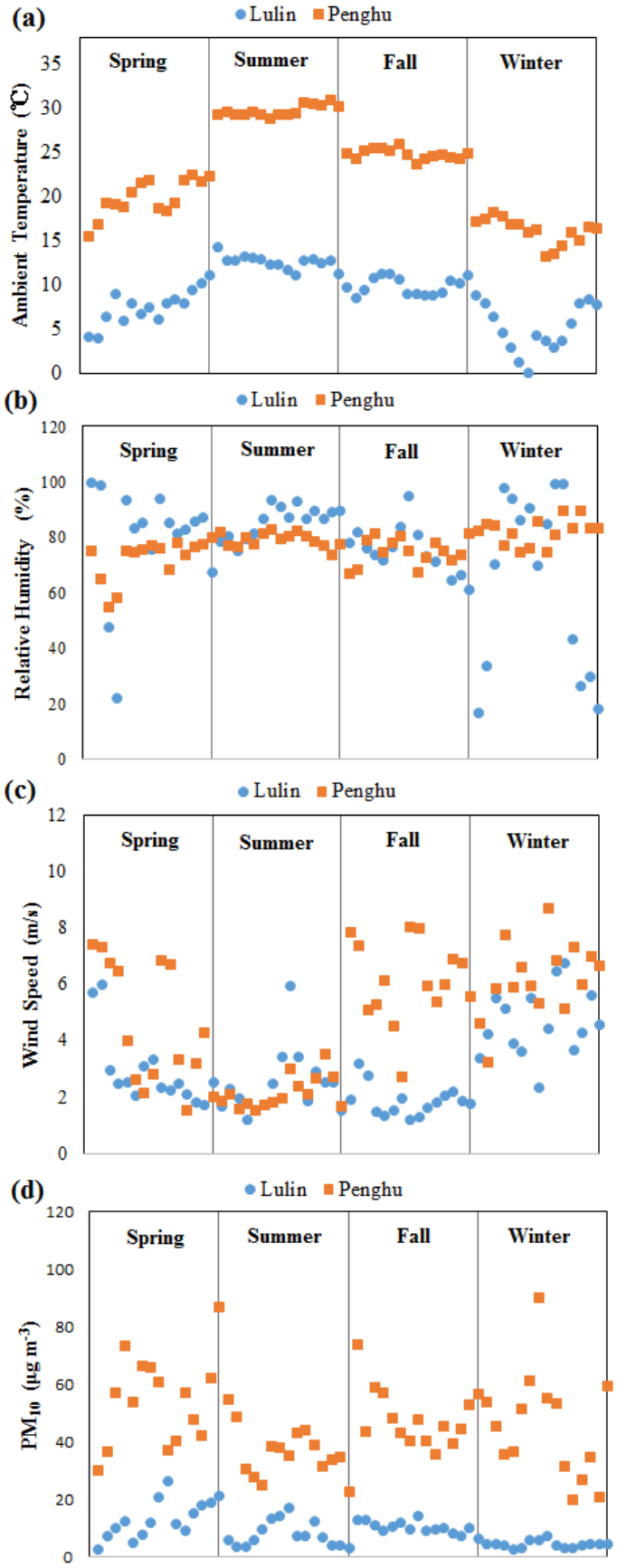

Fig. 3. Seasonal variation of meteorological parameters at two remote monitoring sites for (a) ambient temperature, (b) relative humidity, (c) wind speed, and (d) PM_{10}.

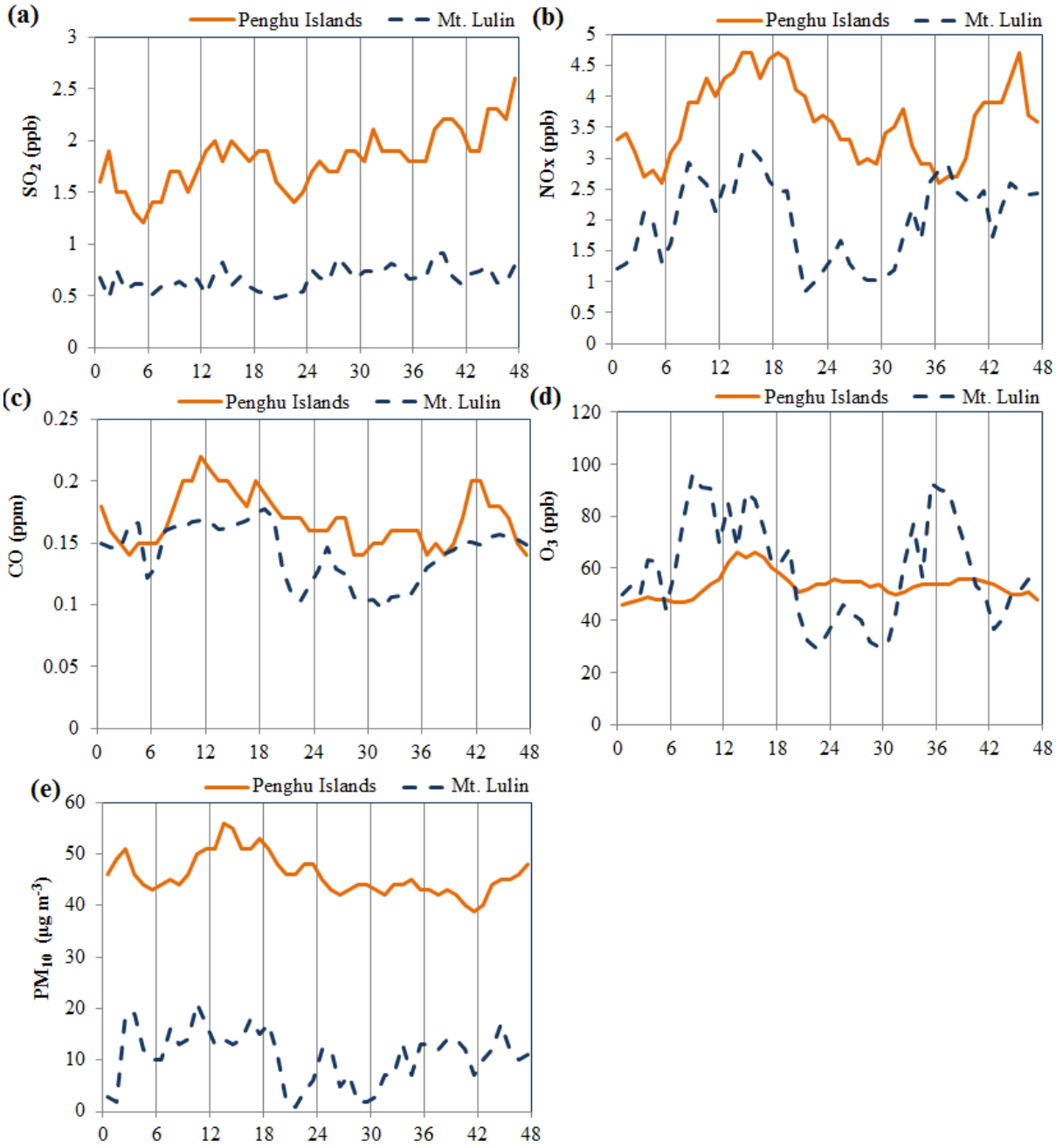

Fig. 4. Hourly variation of air pollutant measured at two remote sites, the Mt. Lulin and the Penghu Islands for (a) sulfur dioxide, (b) nitrogen oxides, (c) carbon monoxide, (d) ozone. (e) PM_{10}. The solid line (—) represents the Penghu Islands and the dash line (- - -) represents the Mt. Lulin.

of mobile and stationary sources. Distance from the emission sources to the two monitoring sites has a significant influence on NO_x concentration since it could react with VOCs and form photochemical products. Thus, the concentration of NO_x at Mt. Lulin was mostly lower than that at the Penghu Islands, which indicated that the influences of emission sources on NO_x concentration at the Penghu Islands were greater than those at Mt. Lulin.

Additionally, the variation of CO concentrations differed, with lower levels at Mt. Lulin compared to the Penghu Islands (Fig. 4(c)). This might be due to the fact that CO is mainly emitted from automobile exhaust. At these two remote sites, there were absolutely no traffic emissions at Mt. Lulin, while there were some mobile sources, including automobiles and fishing boats, near the Penghu Islands site. CO is mainly derived from traffic emissions near the ground, while SO_2 mostly formed by the combustion of sulfur-containing fuels, and emitted from stacks above the ground. Therefore, long-range transport generally governs the concentration of SO_2, while CO concentration is only influenced by atmospheric dispersion and advection. The concentrations of CO at these two remote sites were within the same order of magnitude;

however, for SO_2, the distances from the emission sources to these two remote sites were quite different. As a result, the difference of CO concentrations at these two sites was smaller than that of the SO_2 concentrations. Ozone concentrations observed at the Penghu Islands were generally more stable than those at Mt. Lulin (Fig. 4(d)). Conversely, a great change was observed at the Mt. Lulin site presumably due to the variations in relative humidity and ambient temperature at Mt. Lulin, which caused dramatic changes in ozone concentration.

Low-Frequency Features of Air Pollutant Concentration

The comparison of seasonal concentration of criteria air pollutants is illustrated in Fig. 5; it shows that the seasonal concentrations of CO, SO_2, NO_x and O_3 monitored at Mt. Lulin were mostly smaller than those at the Penghu Islands. The concentrations of SO_2 and NO_x were mostly higher at the Penghu Islands compared to Mt. Lulin, since these air pollutants come mainly from fuel combustion, such as from mobile and stationary sources at the Penghu Islands (Figs. 5(b) and 5(c)). Occasionally, we expect peaks of air pollutants in the spring and winter seasons at the Penghu Islands; however, the concentration levels at Mt. Lulin was relatively stable with almost no peaks.

Concerning the concentration of CO in winter, the Penghu Island station exhibited higher levels, while the Mt. Lulin station presented relatively lower and more stable levels with no significant seasonal variation between the two remote sites. Since CO is mainly emitted from the incomplete combustion of fuel and wastes, it thus relates to mercury emissions.

However, in terms of photochemical pollutants, this study revealed that less significant differences of O_3 were observed between these two remote stations, mostly within an order of magnitude or less (Fig. 5(d)). Since O_3 is a typical secondary pollutant generated during the photochemical reaction occurring in the near-ground level of the troposphere, ozone could be formed under the irradiation of sunlight for a period of time. The place of O_3 occurrence is generally far away from the emission sources of primary pollutants (Lin and Pehkonen, 1999). Consequently, ozone could be also observed at the mountainous sites in the downwind regions.

Discrimination Factor

Linear discriminant analysis (LDA) is closely related to principal component analysis (PCA) and factor analysis in that they both look for linear combinations of variables which best explain the data (Martinez *et al.*, 2001). The discriminant factor describes the level of significant differences between two parameters of interest obtained from the two remote sites. As shown in Fig. 6(a), NO_x and PM_{10} present the principal components, indicating that NO_x and PM_{10} can help us to directly validate the results obtained from the elevated mountain site and the sea-level site. The discriminant factor can be expressed as,

$$DF = 0.08\ C_{PM10} + 0.26\ C_{NOx} - 2.70 \quad (1)$$

where DF is the discriminant factor, as derived from the concentrations of PM_{10}, and NO_x. This equation can distinguish the negative and positive values at the two remote sites for differentiating the source types of air pollutants at Mt. Lulin and the Penghu Islands, respectively. The discrimination results are visualized in Fig. 6(b). In the atmospheric chemistry of air pollution, nitrogen oxides (NO_x) refer specifically to NO and NO_2. They are produced during combustion at high temperature. These two chemicals are important trace species in Earth's atmosphere. In the troposphere, NO_2 is photolyzed by sunlight to form the reactive radical $NO^{\cdot}$. The oxygen atom formed in the second reaction then goes on to form ozone; this series of reactions is the main source of tropospheric ozone. The positive values of the discriminant factor were observed at the Penghu Islands, while the negative values of those were observed at Mt. Lulin. The results indicated that the sources of air pollutants were dominated by the different source origins at these two remote sites.

Atmospheric Mercury Transportation Pattern with Associated Air Pollutant Features

The transportation of atmospheric mercury and its correlation with other criteria air pollutants, with the usage of the high- and low-frequency variations, were found to be very important in understanding the transportation patterns of atmospheric mercury.

In this study, we used the seasonal variation of atmospheric mercury at the two remote sites as an example for the analysis of low-frequency variations, as illustrated in Fig. 7. The higher and lower lines represent the maxima and the minima of the pollutant concentration within a day. Seasonal low-frequency variation of atmospheric mercury between the two remote sites indicated that the variation of atmospheric mercury monitored at Mt. Lulin was higher than that at the Penghu Islands.

Fig. 8 depicts the high-frequency daily variation of atmospheric mercury between the two remote sites. For the concentrations of air pollutants monitored at the Penghu Islands, the diurnal variation of atmospheric mercury was apparently dramatic, while it appeared relatively lower at Mt. Lulin compared to the Penghu Islands. The results further indicated that the concentrations of atmospheric mercury monitored at Mt. Lulin could be treated as the background level, while the Penghu Islands was highly affected by various local sources and cross-boundary transportation, including stationary sources of fuel combustion and biomass burning, as well as mobile sources emitted from automobiles and fishery boats.

Transportation Mechanisms: Background and Scenario Mercury

The Mt. Lulin and the Penghu Island monitoring stations are located in different climatic regions; therefore, the results of comparative parallel analysis between the two remote stations could help us to clarify major mechanisms of atmospheric mercury emitted from the potential sources to the atmosphere. We speculated on the transportation mechanisms of atmospheric mercury at the two remote sites by using the abovementioned analytical results.

In the atmosphere, gaseous elemental mercury (Hg^0) acts

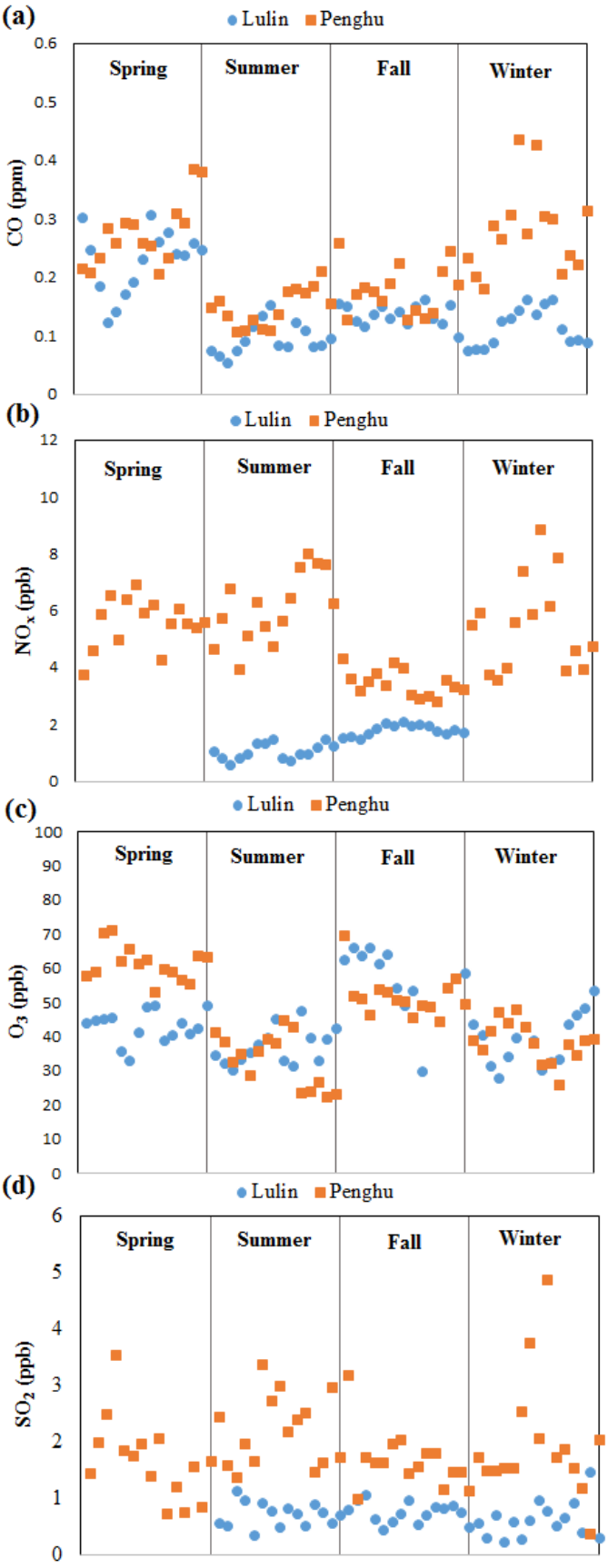

Fig. 5. Seasonal variation of air pollutants at the two remote sites for (a) carbon monoxide, (b) nitrogen dioxide, (c) ozone, and (d) sulfur dioxide.

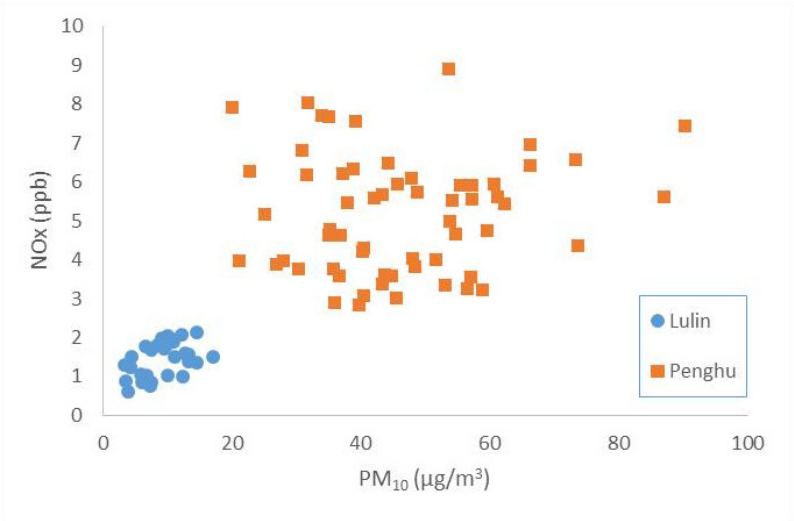

(a)

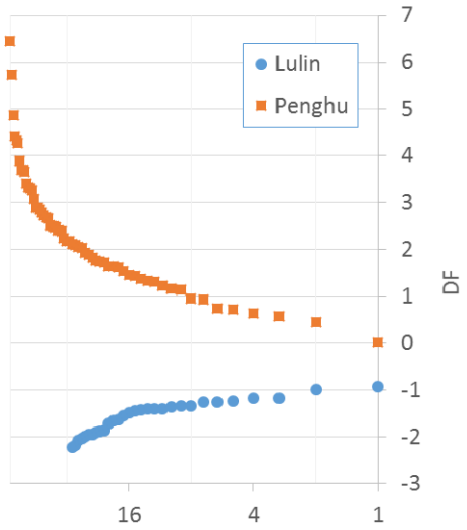

(b)

Fig. 6. (a) Principal component index of, and (b) discriminant factor by NO_x and PM_{10} between two remote sites.

as a valuable and efficient catalyst that can chemically convert carbon dioxide (CO_2) to carbon monoxide (CO) (Feng *et al.*, 2002; Fu *et al.*, 2010; Sommar *et al.*, 2010). As illustrated in Fig. 9, it is clearly observed that there was a good correlation between CO and Hg at low atmospheric mercury concentrations. In this study, the atmospheric mercury monitored at the two remote sites was total gaseous mercury (TGM), including the major portion (> 98%) of gaseous elemental mercury (GEM) and the minor portion (≤ 2%) of gaseous oxidized mercury (GOM) (Poissant *et al.*, 2005; Lindberg *et al.*, 2007; Valente *et al.*, 2007; Bittrich *et al.*, 2011). The partitions of speciated mercury are quite similar elsewhere in the atmosphere all over the world.

The diurnal concentration of atmospheric mercury monitored at Mt. Lulin was relatively stable, while its variation was much more significant at the Penghu Islands. This study revealed that the concentration of atmospheic mercury (1.0–2.0 ng m^{-3}) monitored at Mt. Lulin was close to the North Hemisphere background level (1.4–1.6 ng m^{-3}) of atmospheric mecury, with the major species of gaseous elemental mecury (GEM) (Sheu *et al.*, 2010). The concentration of mercury measured at the Penghu Islands probably came from nearby local sources because it is mainly generated by pollution; it is also known as situational mercury or scenario mercury. Previous research reported that the main ingredient of such scenario mercury was particulate mercury (PHg), and came up with the mechanism of mercury as aerosol trace metals with particle morphology and total gaseous mercury (TGM) in the atmosphere of Oxford, England (Witt *et al.*, 2010).

There is a dramatic change in the concentrations of atmospheric mercury during spring and autumn. This might be attributed to the co-variations of other criteria air pollutants, as illustrated in Fig. 8. There is also a phenomenon of higher PM_{10} concentrations in the spring and autumn observed at the Penghu Islands (Fig. 3(d)).

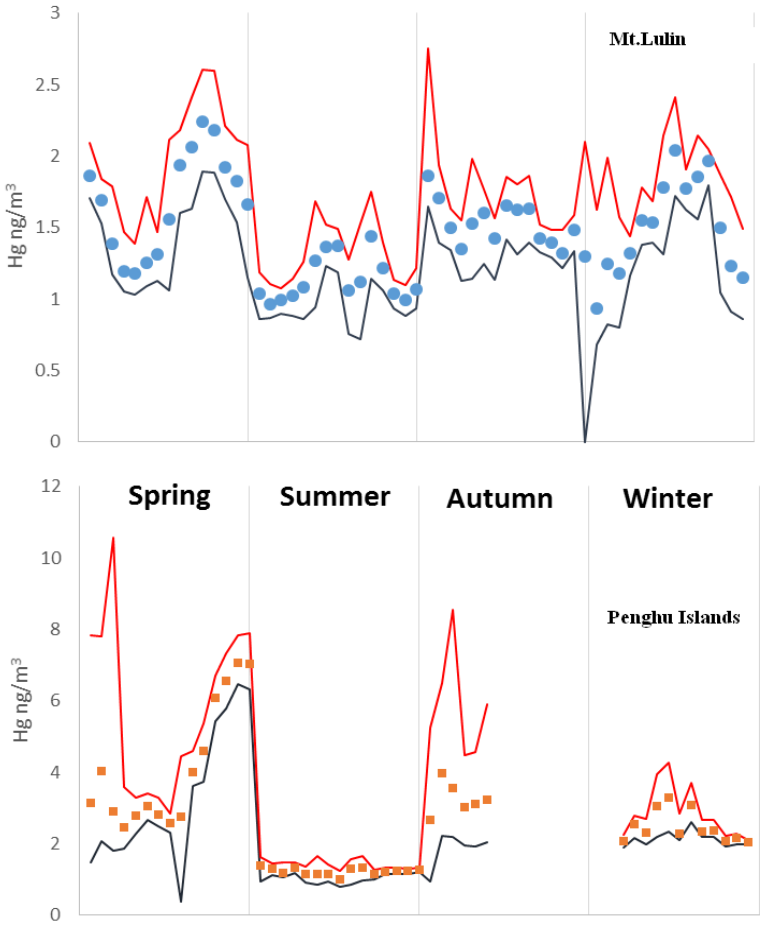

Fig. 7. Low-frequency seasonal variation of atmospheric mercury (TGM) between two remote sites.

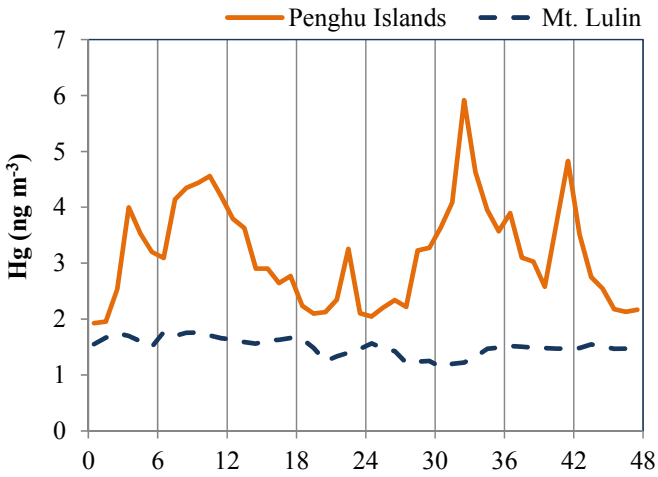

Fig. 8. High-frequency daily variation of atmospheric mercury (TGM). The solid line (—) represents the Penghu Islands and the dash line (- - -) represents the Mt. Lulin.

CONCLUSIONS

The study investigated the correlation patterns of atmospheric mercury and criteria air pollutants associated with meteorological parameters between two remote sites (Mt. Lulin and the Penghu Islands) in the subtropical region, by using the filtering techniques for correlation analysis. The wind direction, wind speed and relative humidity at Mt. Lulin changes drastically, and is more stable at the Penghu Islands. The concentration of each air pollutant monitored at Mt. Lulin was smaller than that at the Penghu Islands, with the exception of ozone concentration. NO_x and PM_{10} comprised

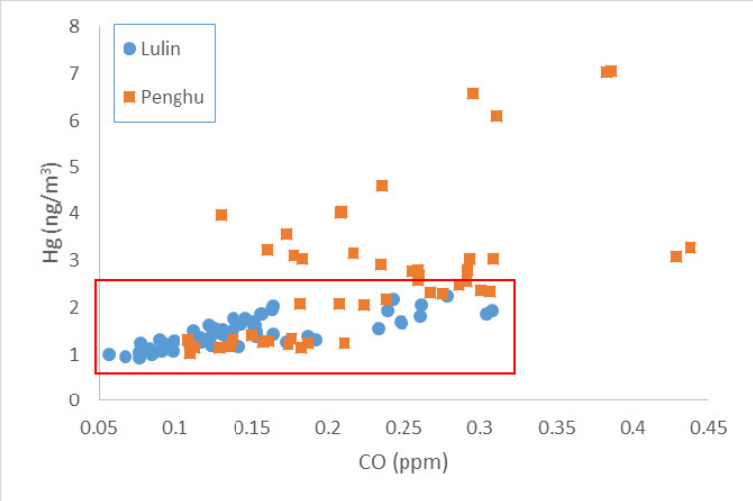

(a) All data

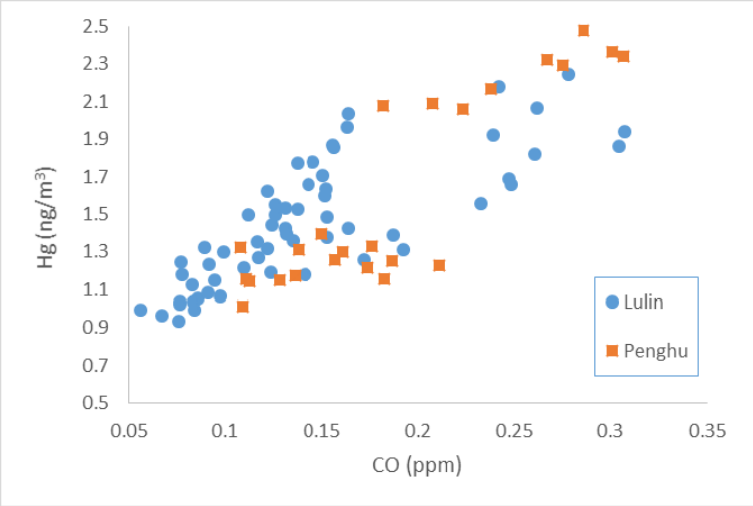

(b) Low concentration

Fig. 9. Linear correlations of atmospheric mercury (TGM) and carbon monoxide (CO) for (a) all data and (b) low concentration. Hg in y-axis represents total gaseous mercury (TGM) including gaseous elemental mercury (GEM) and gaseous oxidized mercury (GOM).

the discrimination index of the atmospheric parameters between the two remote sites, and these two criteria air pollutants were the important factors for distinguishing two clusters of measurement data. For both high- and low-frequency waves, the concentrations of NO_x and PM_{10} show significant differences between the two remote sites. However, ozone concentrations exhibited almost no differences between the two remote sites, implying that the pattern of the formation and transportation of ozone at these two remote sites resulted from similar mechanisms. Moreover, atmospheric mercury had a very good linear correlation with CO. The diurnal variation of Hg concentration was dramatic at the Penghu Islands, while it appeared as low as the North Hemisphere background concentration at Mt. Lulin, indicating that they were not formed via the same mechanism modes. This study thus proposed examining "scenario mercury" and "background mercury" in order to interpret this phenomenon.

ACKNOWLEDGMENTS

This study was conducted under the auspicious of Ministry of Science and Technology (MOST) of Taiwan. The authors would like to express their great appreciation to the Mt. Lulin Meteorological Station of National Central University (NCU) and the Penghu Air Quality Monitoring Station of Taiwan Environmental Protection Administration (TEPA) for providing their measured air quality data and meteorological parameters.

REFERENCES

Bash, J.O. and Miller D.R. (2007). A note on elevated total gaseous mercury concentrations downwind from an agriculture field during tilling. *Sci. Total Environ.* 388: 379–388.

Bittrich, D.R., Chadwick, S.P., Babiarz, C.L., Manolopoulos,

H., Rutter, A.P., Schauer, J.J., Armstrong, D.E., Collett, J. and Herckes, P. (2011). Speciation of mercury (II) and methylmercury in cloud and fog water. *Aerosol Air Qual. Res.* 11: 161–169.

Cheng, H. and Hu, Y. (2010). China needs to control mercury emissions from municipal solid waste (MSW) incineration. *Environ. Sci. Technol.* 44: 7994–7995.

Chuang, M.T., Lee, C.T., Chou, C.C.K., Lin, N.H., Sheu, G.R., Wang, J.L., Chang, S.C., Wang, S.H., Chi, K.H., Young, C.Y., Huang, H., Chen, H.W., Weng, G.H., Lai, S.Y., Hsu, S.P., Chang, Y.J., Chang, J.H. and Wu, X.C. (2014). Carbonaceous aerosols in the air masses transported from Indochina to Taiwan: Long-term observation at Mt. Lulin. *Atmos. Environ*. 48: 507–516.

Ci, Z., Zhang, X., Wang, Z. and Niu Z. (2011). Atmospheric gaseous elemental mercury (GEM) over a coastal/rural site downwind of East China: Temporal variation and long-range transport. *Atmos. Environ*. 45: 2480–2487.

Cole, A.S., Steffen, A., Pfaffhuber, K.A., Berg, T., Pilote, M., Poissant, L., Tordon, R. and Hung, H. (2013). Ten-year trends of atmospheric mercury in the high Arctic compared to Canadian sub-Arctic and mid-latitude sites. *Atmos. Chem. Phys.* 13: 1535–1545

Durnford, D., Dastoor, A., Figueras-Nieto, D. and Ryjkov, A. (2010). Long range transport of mercury to the arctic and across Canada. *Atmos. Chem. Phys.* 10: 6063–6086.

Fang, F.M., Wang, Q.H. and Li, J.F. (2001). Atmospheric particulate mercury concentration and its dry deposition flux in Changchun City, China. *Sci. Total Environ.* 281: 229–236.

Feng, X.B. and Qiu, G.G. (2008). Mercury pollution in Guizhou, Southwestern China — An overview. *Sci. Total Environ.* 400: 227–237.

Fu, X.W., Feng, X.B., Zhu, W.Z, Wang, S.F., and Lu J. (2008). Total gaseous mercury concentrations in ambient air in the eastern slope of Mt. Gongga, South-Eastern fringe of the Tibetan plateau, China. *Atmos. Environ*. 42: 970–979.

Fu, X.W., Feng, X.B, Wang S.F, Rothenberg, S., Shang, L., Li, Z., and Qiu, G. (2009). Temporal and spatial distributions of total gaseous mercury concentrations in ambient air in a mountainous area in southwestern China: Implications for industrial and domestic mercury emissions in remote areas in China. *Sci. Total Environ.* 407: 2306–2314.

Fu, X.W., Feng, X.B., Dong, Z.Q., Yin, R.S., Wang, J.X., Tang, Z.R. and Zhang, H. (2010). Atmospheric gaseous elemental mercury (GEM) concentrations and mercury depositions at a high-altitude mountain peak in south China. *Atmos. Chem. Phys. Discuss.* 9: 23465–23504.

Fu, X.W., Feng, X., Liang, P., Deliger, Zhang, H., Ji, J. and Liu, P. (2012). Temporal trend and sources of speciated atmospheric mercury at Waliguan GAW station, Northwestern China. *Atmos. Chem. Phys.* 12: 1951–1964.

Jen, Y.H., Yuan, C.S., Hung, C.H., Ie, I.R. and Tsai, C.M. (2013). Tempospatial variation and partition of atmospheric mercury during wet and dry seasons at sensitivity sites within a heavily polluted industrial city. *Aerosol Air Qual. Res.* 13: 13–23.

Jen, Y.H., Chen, W.H., Hung, C.H., Yuan, C.S. and Ie, I.R. (2014). Field Measurement of total gaseous mercury and its correlation with meteorological parameters and criteria air pollutants at a coastal site of the Penghu Islands. *Aerosol Air Qual. Res.* 14: 364–375.

Kim, P.R., Han, Y.J., Holsen, T.M. and Yi, S.M. (2012). Atmospheric particulate mercury: concentrations and size distributions. *Atmos. Environ*. 61: 94–102.

Kumari, A., Kumar, B., Manzoor, S. and Kulshrestha, U. (2015). Status of atmospheric mercury research in South Asia: A review. *Aerosol Air Qual. Res.* 15: 1092–1109.

Lee, C.T., Chuang, M.T., Lin, N.H., Wang, J.L., Sheu, G.R., Chang, S.C., Wang, S.H., Huang, H., Chen, H.W., Liu, Y.L., Weng, G.H., Lai, H.Y. and Hsu, S.P. (2011). The enhancement of $PM_{2.5}$ mass and water-soluble ions of biosmoke transported from Southeast Asia over the Mountain Lulin site in Taiwan. *Atmos. Environ*. 45: 5784-5794

Leonardo, R.D., Bellanca, A., Capotondi, L., Cundy, A. and Neri, R. (2007). Possible impacts of Hg and PAH contamination on benthic foraminiferal assemblages: an example from the Sicilian coast, central Mediterranean. *Sci. Total Environ.* 388: 168–183.

Li, T.C., Yuan, C.S., Lo, K.C., Huang, C.H., Wu, S.P. and Tong C. (2015). Seasonal variation and chemical characteristics of atmospheric particles at three Islands in the Taiwan Strait. *Aerosol Air Qual. Res.* 15: 2277–2290.

Lin, C.J. and Pehkonen, S.O. (1999). The chemistry of atmospheric mercury: A review. *Atmos. Environ*. 33: 2067–2079.

Lindberg, S., Bullock, R., Ebinghaus, R., Engstrom, D., Feng, X.B., Fitzgerald, W., Pirrone, N., Prestbo, E. and Seigneur, C. (2007). A synthesis of progress and uncertainties in attributing the sources of mercury in deposition. *Ambio* 36: 19–32.

Liu, F., Cheng H.X., Yang, K., Zhao, C.D., Liu, Y.H., Peng, M. and Li, K. (2014). Characteristics and influencing factors of mercury exchange flux between soil and air in Guangzhou City. *J. Geochem. Explor.* 139: 115–121.

Martinez, A.M. and Kak, A.C. (2001). PCA versus LDA. *IEEE Trans. Pattern Anal. Mach. Intell.* 23: 228–233.

McLachlan, G.J. (2004). *Discriminant Analysis and Statistical Pattern Recognition*. A Wiley Interscience Publication. ISBN 0-471-69115-1. MR 119046.

Nguyen, H.T., Kim M.Y. and Kim, K.H. (2010). The influence of long-range transport on atmospheric mercury on Jeju Island, Korea. *Sci. Total Environ.* 408: 1295–1307.

Pacyna, E.G., Pacyna, J.M., Steenhuisen, F. and Wilson, S. (2006). Global anthropogenic mercury emission inventory for 2000, *Atmos. Environ*. 40: 4048–4063.

Pal, B. and Ariya, P.A., (2004). Gas-phase HO center dot-Initiated reactions of elemental mercury: Kinetics, product studies, and atmospheric implications. *Environ. Sci. Technol.* 38: 5555–5566.

Pfaffhuber, K.A., Berg, T., Hirdman, D. and Stohl, A. (2012). Atmospheric mercury observations from Antarctica:

Seasonal variation and source and sink region calculations. *Atmos. Chem. Phys.* 12: 3241–3251.

Poissant, L., Pilote, M., Beauvais, C., Constant, P. and Zhang, H.H. (2005). A year of continuous measurements of three atmospheric mercury species (GEM, RGM and Hgp) in Southern Quebec, Canada. *Atmos. Environ*. 39: 1275–1287.

Schroedert, W.H. and Munthes, J. (1998). Atmospheric mercury-An overview. *Atmos. Environ*. 32: 809-809.

Sheu, G.R., Lin, N.H., Wang, J.L., Lee, C.T., Ou Yang C.F. and Wang S.H. (2010). Temporal distribution and potential sources of atmospheric mercury measured at a high-elevation background station in Taiwan. *Atmos. Environ*. 44: 2393–2400.

Sheu, G.R. and Lin, N.H. (2013). Characterizations of wet mercury deposition to a remote islet (Pengjiayu) in the subtropical Northwest Pacific Ocean. *Atmos. Environ*. 77: 474–481.

Sheu, G.R., Lin, N.H., Lee, C.T., Wang, J.L., Chuang, M.T., Wang, S.H., Chi, K.H. and Yang C.F. (2013). Distribution of atmospheric mercury in northern Southeast Asia and South China Sea during Dongsha Experiment. *Atmos. Environ*. 78: 174–183.

Slemer, F. and Langer, E. (1992). Increase in global atmospheric concentrations of mercury inferred from measurements over the Atlantic Ocean. *Nature* 355: 434–437.

Sommar, J., Andersson, M.E. and Jacobi, H.W. (2010). Circumpolar measurements of speciated mercury, ozone and carbon monoxide in the boundary layer of the Arctic Ocean. *Atmos. Chem. Phys.* 10: 5031–5045.

Valente, R.J., Shea, C., Humes, K.L. and Tanner, R.L. (2007). Atmospheric mercury in the great smoky mountains compared to regional and global levels. *Atmos. Environ*. 41: 1861–1873.

Wang, D.Y., He, L., Wei, S.Q. and Feng X.B. (2006). Estimation of mercury emission from different sources to atmosphere in Chongqing, China. *Sci. Total Environ.* 366: 722–728.

Witt, M.L.I., Meheran, N., Mather, T.A., De Hoog, J.C.M. and Pyle, D.M. (2010). Aerosol trace metals, particle morphology and total gaseous mercury in the atmosphere of Oxford, UK. *Atmos. Environ*. 44: 1524–1538.

Wu, Y.L., Rahmaningrum, D.G., Lai, Y.C., Tu, L.K., Lee, S.J., Wang, L.C. and Chang-Chien, G.P. (2012). Mercury emissions from a coal-fired power plant and their impact on the nearby environment. *Aerosol Air Qual. Res.* 12: 643–650.

Yuan, C.S., Sau, C.C. and Chen, M.C. (2004a). Influence of Asian dusts on the physicochemical properties of atmospheric aerosols in Taiwan district – Using the Penghu islands as an Example. *Particuology* 2: 144–152.

Yuan, C.S., Sau, C.C., Chen, M.C., Hung, M.H., Chang, S.W. and Lin, Y.C. (2004b). Mass concentration and size-resolved chemical composition of atmospheric aerosols sampled at Pescardores Islands during Asian dust storm periods in the years of 2001 and 2002. *Terr. Atmos. Oceanic Sci.* 15: 857–879.

Received for review, July 14, 2015
Revised, February 8, 2016
Accepted, March 10, 2016